HHS Public Access

Author manuscript

Nanomedicine. Author manuscript; available in PMC 2018 January 01.

Published in final edited form as:

Nanomedicine. 2017 January ; 13(1): 253–262. doi:10.1016/j.nano.2016.09.001.

Coated protein nanoclusters from influenza H7N9 HA are highly immunogenic and induce robust protective immunity

Li Wang[1], **Timothy Z. Chang**[2], **Yuan He**[1], **Jong R. Kim**[1], **Shelly Wang**[1], **Teena Mohan**[1,2], **Zachary Berman**[1,3], **S. Mark Tompkins**[4], **Ralph A. Tripp**[4], **Richard W. Compans**[1], **Julie A. Champion**[2], and **Bao-Zhong Wang**[1,3,*]

[1]Department of Microbiology and Immunology, Emory University School of Medicine. 1518 Clifton Rd, 5th floor, Claudia Nance Rollins Building, Atlanta, GA 30322, USA

[2]Georgia Institute of Technology, School of Chemical & Biomolecular Engineering. L1236 Ford ES&T, Atlanta, GA 30332, USA

[3]Center for Inflammation, Immunity & Infection, Georgia State University Institute for Biomedical Sciences. 716 Petit Science Center, 100 Piedmont Ave SE. Atlanta, GA 30303, USA

[4]Animal Health Research Center, University of Georgia. 111 Carlton Street, Building 1077, Athens, GA 30602, USA

Abstract

Recurring influenza viruses pose an annual threat to public health. A time-saving, cost-effective and egg-independent influenza vaccine approach is important particularly when responding to an emerging pandemic. We fabricated coated, two-layer protein nanoclusters from recombinant trimeric hemagglutinin from an avian-origin H7N9 influenza A virus as an approach for vaccine development in response to an emerging pandemic. Assessment of the virus-specific immune responses and protective efficacy in mice immunized with the nanoclusters demonstrated that the vaccine candidates were highly immunogenic, able to induce protective immunity and long-lasting humoral antibody responses to this virus without the use of adjuvants. Because the advantages of the highly immunogenic coated nanoclusters also include rapid productions in an egg-independent system, this approach has great potential for influenza vaccine production not only in response to an emerging pandemic, but also as a replacement for conventional seasonal influenza vaccines.

Graphical abstract text

Coated protein nanoclusters were fabricated from recombinant trimeric HA protein of H7N9 influenza virus by desolvation followed by crosslinking. The resulting nanoclusters were highly immunogenic, able to induce high levels of antibody responses conferring immune protection against live virus challenge in mice.

*Corresponding author: Center for Inflammation, Immunity & Infection, Georgia State University Institute for Biomedical Sciences. 100 Piedmont Ave SE, Atlanta, GA 30303, USA. bwang23@gsu.edu, Phone: 404-413-3652, Fax: 404-413-3580.

Conflict of interest statement: There are no known conflicts of interests.

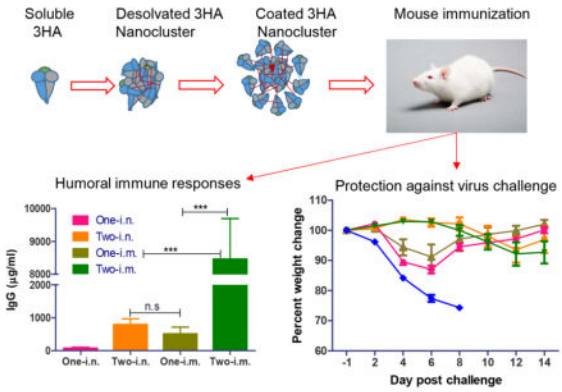

Keywords

Influenza vaccine; pandemic influenza; protein nanoclusters

Introduction

Influenza A virus infection remains one of the leading causes of morbidity and mortality worldwide, and vaccination is the best approach to prevent influenza (1, 2). In early 2013, a novel avian-origin influenza A H7N9 virus was reported to have infected humans in eastern China. According to the WHO's report, as of February 23, 2015, 571 human cases of influenza A H7N9 infection, including 212 deaths, were reported worldwide, which is the highest mortality rate (37%) attributed to H7 infections to date (3–5). It was reported that the human population is immunologically naïve to the H7N9 virus (6, 7). The potential for viral adaptation that would facilitate person-to-person transmission remains a major concern (8). Critically, human clinical trials with inactivated H7 avian influenza vaccines have indicated that the H7 virus is poorly immunogenic (9, 10). Conventional inactivated H7N9 vaccines or VLP vaccines were demonstrated to be poorly immunogenic in laboratory animals, requiring multiple/high doses or needing to be co-administered with adjuvants for complete protection (6, 8, 11, 12). In fact, the manufacture of conventional egg-based vaccines can require at least 6 months to supply large enough quantities to immunize global populations (13, 14). There are concerns about the safety of these vaccines in individuals with egg allergies (15). A more effective vaccine which requires a shorter production period and is egg-independent, is necessary for not only continued preparedness in combating emerging pandemics, but also the replacement of the conventional seasonal vaccines (16). Due to the importance of Hemagglutinin (HA) in both the immunogenicity of conventional influenza vaccines and the viral entry function, recombinant HA-based subunit vaccines have long been investigated, but some weaknesses including low immunogenicity have to be overcome before they can replace current virus-based vaccines (17–20).

Previously, we reported an effective vaccine design with influenza virus M2e proteins assembled directly into nanoclusters under gentle fabrication conditions (21). Different from other particulate vaccine platforms, these nanoparticles were almost entirely generated from the antigenic protein of interest; thus the nanoparticles had a high antigen load and exhibited

high immunogenicity (21). In this study, we refined the nanocluster designs to assemble trimeric H7N9 HA proteins into nanoclusters with an additional HA protein layer coated on the particle surface by a chemical crosslinking process. The potentials of the coated nanoclusters as a new generation of influenza vaccine were determined.

Methods

Ethics Statement

This study was carried out in strict accordance with the recommendations in the Guide for the Care and Use of Laboratory Animals of the National Institutes of Health. All mouse studies were approved by the Emory University Institutional Animal Care and Use Committees (IACUCs) with protocol numbers of 2001659. Female BALB/C mice (6–8-week old) were purchased from the Jackson Laboratory and housed in the animal facility at Emory University. Immunization, sampling and bleeding were performed under anesthesia that was induced by light inhalation of isoflurane to reduce mouse suffering.

Cell lines and viruses

Sf9 insect cells and MDCK cells were cultured as described previously (21). JAWS II murine dendritic cells were grown in alpha MEM containing 10% FCS and 5 ng/ml murine GM-CSF at 37°C. Mouse-adapted influenza virus A/Anhui/1/2013 (H7N9) was prepared as lung homogenates from intranasally (i.n.) infected mice. The LD_{50} (50% lethal dose) was calculated by the method of Reed and Muench (22).

Purification and characterization of recombinant hemagglutinin proteins

H7N9 A/Anhui/2013 HA cDNA (Accession number EPI439507 in GISAID EpiFlu database) was used to generate HA expressing constructs. The monomeric HA (1HA) construct was generated by introducing a 6-histidine-tag (his-tag) coding sequence followed with by a stop codon upstream of the transmembrane domain coding sequence. A trimeric form of GCN4 sequence-stabilized trimeric HA (3HA) construct was generated as previously described (16). Recombinant baculoviruses (rBVs) expressing 1HA and 3HA were generated and soluble 1HA and 3HA recombinant proteins were purified from the insect cell protein expression as previously described (16).

Bis [sulfosuccinimidyl] (BS3) crosslinking

The monomeric or trimeric status of purified HA proteins was determined using the soluble Bis [sulfosuccinimidyl] (BS3) crosslinker (Pierce-Rockford, IL) in a crosslinking reaction to fix the polymeric structures of proteins followed with SDS-PAGE, as described previously (16).

Nanocluster fabrication

Desolvation 3HA nanoclusters were generated as previously described with modification (21). In brief, the solution contained 1.6 mg/ml of protein in PBS and was desolvated with a 4:1 volume ratio of ethanol to protein solution. The particles were collected by centrifugation, and resuspended in sterile PBS with sonication. To coat an additional layer of

3HA molecules onto the 3HA nanoclusters, 800 μg of soluble 3HA protein was added at a concentration of 1.6 mg/ml to 480 μg desolvated 3HA nanoclusters and an amine crosslinking reaction was performed using 3 mM 3,3′-Dithiobis[sulfosuccinimidylpropionate (DTSSP, Thermo Scientific, Waltham, MA) for 12 hours while stirring to stabilize the nanoparticles. Coated nanoclusters were collected by centrifugation, and protein concentration was measured by a BCA assay according to the manufacturer's instructions (Thermo Scientific) to estimate the total protein content in nanoparticles. Dynamic light scattering (DLS) was performed in PBS with a Malvern Zetasizer Nano ZS (Malvern Instruments, Westborough, MA) to assess nanoparticle size distributions. For scanning election microscopy studies, coated 3HA nanoparticles were resuspended in water, dried, and sputter coated with carbon prior to visualization with a Zeiss Ultra60 FE scanning electron microscope at 5.0 kV.

In vitro assays for inflammation and maturation of dendritic cells

JAWS II murine dendritic cells (DCs, passages 6–15) were plated at 10^5 cells/ml in 24-well plates for *in vitro* measurement of inflammation and maturation responses. After 24 hours of incubation, cells were stimulated with 10 μg/ml of soluble 3HA or coated 3HA nanoclusters in fresh complete media. A final concentration of 1 μg/ml of LPS was used as a positive control treatment. TNF-α was assessed in supernatants after 6 hours of stimulation by using ELISA kits (R&D Systems, Minneapolis, MN).

Expression of a cell surface marker for DC maturation, CD86, was assessed by flow cytometry after 24 hours of stimulation. Fc receptors were blocked by TruStain fcX (Biolegend) for 10 minutes on ice. Cells were then incubated with PE-conjugated rat anti-mouse CD86 (clone GL-1) or isotype control (clone RTK2758) antibodies for 30 minutes on ice. After washing two times, cells were fixed with 1% paraformaldehyde and analyzed with a BD Accuri C6 flow cytometer (BD Biosciences, San Jose, CA). Data were analyzed with FlowJo software (FlowJo LLC, Ashland, OR). A duplicative assay was performed.

Immunization, sample collection and challenge

Mice were immunized with either soluble HA bound to alum or HA nanoclusters. For soluble HA immunization, mice were vaccinated twice with 100 μl vaccine mixture containing 2 or 10 μg of 1HA or 3HA soluble protein and Imject Alum Adjuvant (Thermo Scientific) via intramuscular (i.m.) administration. To make the vaccine mixture, a total volume of 50 μl Imject Alum was added dropwise to 50 μl HA protein solution to make the final volume ratio of 1:1. The mixing was lasted for 30 min prior to the immunization, as recommended by the manufacturer. For nanocluster vaccination, mice were immunized with 10 μg of nanoclusters once or twice (with a 4-week interval) via i.m. (in 100 μl PBS) or i.n. (in 25 μl PBS) administration. Blood samples were collected at 3 weeks after priming and boosting. Four weeks after priming or boosting immunization, mice were challenged i.n. with $10xLD_{50}$ of mouse-adapted A/Anhui (in 25 μl PBS). Body weight loss and survival rates were monitored daily for 14 days post infection (p.i.). Weight loss of ≥25% was used as the endpoint at which mice were euthanized according to IACUC guidelines.

Hemagglutination inhibition assay, neutralization assay and antibody ELISA

Hemagglutination inhibition (HAI) and neutralization assays were conducted using diluted sera and pseudotyped virus expressing A/Anhui HA and NA. Recombinant H7N9 pseudovirus was produced as previously described (23) with modification. In brief, 10^7 293T cells were co-transfected with lentivirus vector pNL4-3-Luc R-E- (10 μg DNA), pVKD-HA (5 μg DNA) and pVKD-NA (5 μg DNA). Pseudoviruses were harvested from cell culture supernatants at 48 hours. The median (50%) tissue culture infective dose ($TCID_{50}$) was determined by infection of MDCK cells with serially diluted pseudoviruses and calculated according to the method of Reed and Muench (22), and the infectivity was determined by measuring the relative luciferase activity (RLA). The HAI assay was performed using 2-fold stepwise diluted sera and 1% horse erythrocytes with 8 hemagglutination units (HAU) pseudotyped viruses. For neutralization assays, heat-inactivated (56 °C for 30 min to inactivate complement) immune sera were 2-fold stepwise diluted and mixed with 200-fold $TCID_{50}$ pseudoviruses at a final volume of 100 μl at 37°C for 1 hour; then the mixture was added to MDCK cell monolayers. The neutralizing antibody titers were determined as the serum dilutions that resulted in >50% reduction of RLA. HA-specific antibody (Ab) titers in immune sera were determined by ELISA using 3HA (1 μg/ml) as coating antigens as described previously (21, 24).

Statistical analysis

Comparisons among vaccinated groups were performed using a one-way ANOVA followed by Bonferroni's multiple comparison post-test. Comparison of survival rate was performed using the Log-rank (Mantel-Cox) test. The analyses were done by using GraphPad Prism version 5.00 for Windows (GraphPad Software, San Diego, CA). P-values of less than 0.05 (*, $p<0.05$) were considered to be statistically significant. **, $p<0.005$; ***, $p<0.001$; n.s., $p>0.05$.

Results

Characterization and immunogenicity of recombinant H7N9 HA proteins purified from recombinant baculovirus protein expression

We previously reported that recombinant trimeric hemagglutinin (3HA) from an H3N2 virus was highly immunogenic (16). In order to test if the immunogenicity of H7N9 HA can be improved by trimerization, genes encoding both monomeric (1HA) and trimeric (3HA) HA proteins of A/Anhui were constructed (Figure 1A), and the two recombinant proteins were purified. As shown in Figure 1B, the Western blotting analysis confirmed the correctness of the purified 1HA and 3HA, indicated by the right molecular weight as calculated from their amino acid composition (lanes 1 and 2). As shown in Figure 1B, after cross-linking with BS3, 3HA showed a major band of approximately 200 kD, which is 3-fold higher than that without crosslinking, indicating that the purified 3HA protein is trimeric (lanes 4, 6, and 8). In contrast, 1HA remained as a single band of about 70 kD after the BS3 crosslinking reaction (lanes 3, 4, and 5). These data demonstrated that both monomeric and trimeric forms of recombinant proteins were successfully purified from rBV-derived protein expression in insect cells.

Next, we performed an immunization study in mice to determine whether 3HA is more immunogenic than 1HA. Four groups of mice were vaccinated twice (4-weeks apart) with a 2 μg or 10 μg dose of 1HA or 3HA in the presence of alum via the intramuscular (i.m.) route. Four weeks after boost immunization, all animals were challenged with a highly lethal dose ($10xLD_{50}$) of A/Anhui and then monitored for morbidity (percent body weight change) and mortality (percent survival). Mice that received PBS plus alum (negative controls) all died by day 6 (Figure 1C). Whereas 100% of mice that have received 2 μg of 1HA eventually died, 30% of mice vaccinated with 10 μg of 1HA were able to survive the challenge with recovery of body weight by day 12 to 14 (Figure 1C and 1D). Interestingly, animals vaccinated with 3HA lost less body weight with 58% survival (5/12 mice died) in the low dose group and more than 92% survival (1/12 mice terminated) in the high dose group (Figure 1C). Therefore, these data demonstrate that although neither 1HA and 3HA in these experimental settings provided complete protection, 3HA was much more immunogenic than 1HA, showing significantly more potential for subsequent nanocluster vaccine studies.

Generation and characterization of coated nanoclusters from H7N9 3HA

We have previously reported that nanoparticle vaccines generated by desolvation of M2e protein solution elicited broadly cross-protective immune responses in mice (21). This approach is unique, in that vaccine candidates are almost entirely composed of antigens of interest, and do not include any vehicles or vectors. In order to further improve the immunogenicity of the H7N9 3HA vaccine, we generated 3HA nanoclusters by desolvation (Figure 2A, I). In terms of the interaction of HA with its cell surface receptors, 3HA nanoclusters are multivalent, similar to influenza virions. However, when we measured the hemagglutination activity (HA titer) of 3HA nanoclusters with a standard HA titer assay (25), we found that these nanoclusters displayed low ability to agglutinate chicken red blood cells (HA titer was only 8 from a starting protein concentration of 50 μg/ml). Soluble 3HA showed a HA titer of 256. Considering that in the desolvation process to fabricate nanoclusters, 3HA molecules on the surfaces of nanoclusters have a much longer time in contact with the solvent ethanol, and this extended contact may account for the low HA activity of the nanoclusters because these protein molecules may have partially lost their structures. However, the surface HA proteins are most important to the immunogenicity of these nanoclusters due to the fact that they may function as ligands to bind to HA surface receptors and facilitate the uptake of nanoclusters to immune cells by receptor-mediated endocytosis.

In order to produce nanoparticles with high HA titers, an additional layer of 3HA molecules was coated onto the surfaces of desolvated 3HA nanoclusters by a crosslinking reaction to fabricate coated 3HA protein nanoclusters (two-layer nanoclusters; Figure 2A, II). Scanning electron microscopy (SEM) of dehydrated nanoparticles showed that particulates were relatively spherical (Figure 2B and 2C). Dynamic light scattering (DLS) analysis of the nanoparticles indicated the presence of a single, reproducible population distribution with an average hydrodynamic diameter of 273 nm (Figure 2D). The nanoclusters in SEM images appeared smaller than by DLS, indicating that the particles contained significant amounts of water in their normal, hydrated state. The zeta potential of the coated nanoparticles was

−l9.8 ± 0.726, as expected since the zeta potential for soluble 3HA protein is −l 8.74±0.601. These coated 3HA nanoparticles showed high HA activity (the HA titer was 512 with a starting protein concentration of 50 μg/ml), which was 64-fold higher than the 3HA desolvation nanoclusters (HA titer of 8) without the coated layer.

Next, we tested if the coated nanoclusters could be engulfed by dendritic cells (DCs), and if this uptake could stimulate DC maturation by using the JAWS II murine DC cell line. As shown in Figure 2E, treatment with coated 3HA nanoparticles upregulated CD86 expression, as revealed by the enhanced fluorescent intensity (Orange curve). As a positive control, LPS induced a high level of surface CD86 expression on JAWS II cells (Blue curve in Figure 2E). Cells treated with PBS or soluble 3HA protein showed background levels of CD86 expression. In addition, TNF-α production from JAWS II cells was also significantly increased at 6 hours after the coated nanoparticle treatment (Figure 2F), but neither 3HA protein nor PBS treatments resulted in significant increases. These *in vitro* data indicated that coated 3HA nanoparticles can be taken in by DCs, and consequently stimulate DC maturation.

Coated 3HA nanoclusters induced humoral immune responses

It is known that HA-specific antibody responses are the main correlates in providing immune protection by conventional influenza vaccines (18, 26, 27). Serum samples at 3 weeks after prime or boost immunization were analyzed for HA-specific IgG titers in this study. The results in Figure 3 demonstrated that two immunizations with coated 3HA nanoclusters induced robust serum antibody responses in mice by either i.m. or i.n. routes (Two-i.m. or Two-i.n.). Two i.m. immunizations with the nanoclusters resulted in increased levels of HA-specific IgG in immune sera (8456 μg/ml) when compared to the two i.n. immunizations (784 μg/ml) or one i.m. delivery (500 μg/ml) (Figure 3A, $p<0.001$). Although mice received two i.n. immunizations showed higher levels of HA-specific IgG than mice received one i.n. immunization, their antibody levels were significantly lower than the levels found in mice that received two i.m. vaccinations. These results demonstrated that coated 3HA nanoclusters were highly immunogenic, able to induce robust humoral antibody responses by either i.m. or i.n. routes in mice, and that i.m. vaccination elicited higher serum antibody titers than the i.n. route.

Subsequently, the levels of IgG1, IgG2a, and IgG2b specific to HA were also evaluated by ELISA (Figure 3B–D). Similar to the HA-specific total IgG data, two immunizations via the i.m. route dramatically increased HA-specific IgG subclasses when compared to a single dose immunization. Also, a significant difference in HA-specific IgG subclasses was observed in mice that received i.m. *vs.* i.n. vaccination after boost immunizations. Interestingly, mice from all four groups vaccinated with nanoparticles showed much higher IgG1 levels when compared to IgG2a or IgG2b levels, suggesting that coated 3HA nanoparticles induce Th2-biased antibody responses by either the i.m. or i.n. routes, although i.m. immunization induced significantly higher levels of the different IgG subtypes than i.n. immunization.

3HA coated nanocluster immunization induced high hemagglutination inhibition and virus neutralization titers, and better protection of mice from lethal viral challenge

Protective immune responses are commonly reflected by the presence of protective antibodies conferring hemagglutination inhibition (HAI) and viral neutralization in immune sera (18, 27). As an assay to measure the ability of antibodies in sequestering the viral recognizing and binding to host cell receptors and the subsequent blocking viral infection, HAI activity has been recognized as a correlate of protection (28). According to FDA guidelines, an HAI titer greater than or equal to 40 is an essential immunological parameter needed to accurately predict protection from natural infections (29). In contrast to HAI as an indicator for antibody responses to the membrane-distal receptor-binding area in HA protein, antibody neutralization titers of immune sera reflect all antibodies involved in neutralizing virus infectivity, which include antibodies that may recognize the membrane-proximal regions in HA. As demonstrated in Figure 4A and 4B, two immunizations by either the i.m. or i.n. routes induced higher levels of serum HAI and neutralization titers than by one immunization alone. In particular, two i.m. immunizations elicited significantly higher HAI titers and neutralization activity (7-fold higher neutralization activity and 44-fold higher HAI titers) compared to one i.m. immunization only ($P<0.001$), demonstrating the importance of the role of a boosting immunization. Also, the HAI and viral neutralization results were consistent with the high antibody levels shown in Figure 3. However, the boosting effect of antibody responses was much lower in the i.n. route. As shown in Figure 4A and 4B, two i.n. immunizations with coated 3HA nanoclusters induced only 2-fold higher viral neutralizing activity than one priming vaccination ($P<0.05$), and the HAI titer after the boosting immunization only showed a moderately higher response than one i.n. immunization ($P>0.05$). In terms of the HAI and neutralization titers of immune sera, one i.m. immunization induced comparable levels to two i.n. immunizations ($P>0.05$). These results demonstrated that the i.m. route of immunization with coated 3HA nanoclusters was more effective in inducing protective humoral antibody responses.

To address if the coated 3HA nanocluster-induced immune responses conferred protection, immunized mice were infected with $10xLD_{50}$ of mouse-adapted A/Anhui/1/2013 (H7N9) influenza virus intranasally at week 4 for single-dose groups or week 8 for the two immunization groups. As seen in Figure 4C and 4D, naïve mice died on days 6–8 post-challenge, with over 25% body weight loss. In contrast, all vaccinated mice were completely protected from lethal challenge with live virus except for mice in the single-dose i.n. vaccination group which showed partial protection with an 85% survival rate (Figure 4C).

Notably, mice that received two vaccinations via either the i.m. or i.n. routes were fully protected and did not exhibit any bodyweight loss (Figure 4C and 4D). Mice in the one i.m. immunization group all survived the challenge as well, but showed slight bodyweight loss (8%). Moreover, even the single i.n. immunization, which provided partial protection to mice, also clearly decreased signs of morbidity as indicated by the limited 12% loss in body weight on day 6 post-challenge with rapid recovery of body weight afterwards (Figure 4D). These results demonstrate that vaccination with 3HA coated nanoparticles induces protective immunity in mice against lethal challenge with live H7N9 influenza viruses, and that i.m.

immunization with 3HA coated nanoclusters provided better immune protection than the i.n. route in mice.

Coated H7N9 3HA nanoparticles elicit long-term humoral immune responses

We determined whether coated 3HA nanocluster vaccination could induce long-lasting protective antibody responses. As shown in Figure 5, IgG titers were maintained at comparable levels after 3 months for i.m. groups ($P>0.05$), while after 6 months, an approximate 30% decrease in IgG titers was observed ($P<0.05$). In contrast, IgG titers dropped significantly in three months in the two i.n. immunization group ($P<0.05$), and a 50% decrease was seen in 6 months ($P<0.001$). Interestingly, for both the two i.m. and i.n. immunization groups, HAI and neutralization titers did not show significant decreases over a period of 6 months, although their IgG levels dropped as described above (Figure 5B and 5C). This demonstrates that two immunizations were highly effective in inducing protective antibodies which conferred durable HAI activity and viral neutralization. In contrast, serum HAI and neutralization titers in the one i.m. immunization group dropped significantly, although the IgG titers were comparable for the two i.n. and one i.m. immunization groups. The results demonstrate that the coated 3HA nanoparticles induce long-lasting protective humoral immune responses in a priming/boosting immunization strategy in mice, in particular via the i.m. route.

Discussion

A rapid and safe alternative to the conventional virus-based influenza vaccines is critical in an response to an emerging pandemic (30). In this study, we produced rBV-derived soluble trimeric HA from an avian-origin H7N9 virus. A C-terminal fusion with the GCN4 trimerization heptad repeat to stabilize the trimeric structure of the secreted HA was demonstrated not only to resemble the native trimeric structure of the protein but also to increase its immunogenicity (16). We previously demonstrated that protein nanoclusters directly assembled from tetrameric M2e by a desolvation process induced enhanced antibody responses (21). We further refined the protein nanoparticle design to generate two-layer protein nanoclusters from the H7N9 3HA by coating an additional layer of the protein molecules onto the surface of the desolvated 3HA nanoclusters. The coating of the H7N9 3HA protein to the surfaces of the desolvation particles was proposed to increase immunogenicity, since it can closely mimic the natural orientation of this viral surface protein. The results demonstrate that the resulting particles successfully induced higher levels of humoral HA-specific antibody responses, conferring complete protection against H7N9 virus lethal challenge after two i.m. or i.n. immunizations or just one i.m. immunization.

The low immunogenicity of H7N9 has become a significant limitation towards producing an efficacious vaccine and meeting the goal of increased preparedness for a potential pandemic (31, 32). Several approaches have aimed to improve the immunogenicity of vaccine candidates including the use of high doses, multiple immunizations, and the utilization of adjuvants (33, 34). The disadvantages posed by these approaches are evident when discussing a possible emerging influenza pandemic: reducing vaccine recipient numbers and

a limited number of adjuvants available at this time (34). Trimeric HA nanoclusters showed high immunogenicity in inducing protective immunity without the use of any adjuvant, as demonstrated by our results. In addition, the approach has displayed advantages not only in the enhanced immunogenicity of the coated nanocluster vaccines, but also in both safety and manufacturing. Due to the process of desolvation followed with a crosslinking coating process as deployed to generate 3HA nanoclusters, these nanoparticles were almost entirely antigenic proteins except for a tiny amount of small crosslinking molecules. Fixation by a reducible crosslinker endows the protein nanoparticles with the ability to release individual proteins after their uptake into the reducing intracellular environment. The protein feature of these nanoparticles bypasses the safety concerns of other nanoparticulate platforms, including both organic and inorganic nanoparticle systems, which have shown potential toxicity (35, 36).

Our data indicate that the Th2 response is the major response to coated nanocluster immunization since serum IgG1 accounts for the majority of the total IgG response. Unlike Th1 CD4 T cell response which confers anti-viral effect by secreting antiviral molecules and stimulating cellular effect to kill infected cells, Th2 CD4 T cells effect by helping B cell differentiation and proliferation to produce better antibody response, particularly IgG1 response. Antibodies tightly binding to virus surface antigens, such as influenza HA, may block the virus recognition to its host cell surface receptors thus directly neutralize viruses. Previous reports have shown that vaccination with soluble trimerized HA proteins induced a balanced Th1/Th2 response, so it is not clear whether this skewed Th2 response is H7N9 HA antigen dependent or due to the adjuvant effect of the nanoparticles themselves. The induced serum IgG showed a similar pattern for both the i.n. and i.m. vaccinated groups: the primed and boosted mice showed about 10-fold higher IgG when compared to the mice immunized with a single dose, but the amount of IgG induced in the i.m. immunized mice were much higher (~10 fold) than the i.n. vaccinated mice. It is interesting that although the IgG levels were highly variable, the intranasal group exhibited similar weight loss rates when compared to the intramuscular group. It is possible that vaccination through the i.n. route can also induce a mucosal immune response, which may contribute to the protective immunity. Therefore, although the intranasal group induced a much lower level of serum IgG, it still displayed similar protection efficiency to the intramuscular group.

For viral infection initiated at mucosal sites, such as influenza virus, antigen-specific mucosal immunity is thought to be efficient in blocking the initiation of an infection, thus inhibiting its progression into a systemic infection (37, 38). Our previous studies demonstrated that influenza VLP vaccines or M2e nanocluster vaccines induced robust mucosal immune responses, conferring better protection via the i.n. route than by i.m. immunization. Results from our current studies showed that H7N9 3HA nanoclusters induced significantly better immune protection in live viral challenge through i.m. immunization over the i.n. route. As demonstrated previously, nanoparticle and VLP sizes have a dramatic influence on their immunogenicity when utilizing different administration routes (39). Relatively smaller sizes of particulate vaccines are favorable with M cells, the cells specialized in antigen-sampling in mucosal epithelia tissues, as M cells take in the particles and release them basolaterally for interaction with other mucosal immune cells to stimulate antigen-specific immune responses (39, 40). Compared to the previous VLPs

(about 80–120 nm in diameters) or nanoclusters (an average of diameter of 170 nm), the current 3HA nanoclusters were larger with an average size of 273 nm (21, 24). This larger size may account for the lower levels of protective immunity seen after i.n immunization. Therefore, it is important to optimize the size of the coated 3HA nanoclusters for i.n. immunization in the future, so that vaccines can be developed using needle-free approaches, such as a nasal spray, for administration of influenza vaccines.

In conclusion, the coated 3HA nanoparticles are promising influenza vaccine candidates. The mechanisms of the enhanced immunogenicity over soluble proteins include the high antigen density presented on particle surfaces and the increased capability of internalization by APCs. While the 3HA nanoparticles were not expected to easily penetrate the extracellular matrix to be drained to the LNs directly as those <100 nm, they will be eventually scavenged by local DCs. High immunogenicity along with production convenience, this approach shows great promise to replace the current time-consuming, egg-dependent production of seasonal influenza vaccines.

Acknowledgments

The study was supported by the National Institute of Allergy and Infectious Diseases of the National Institutes of Health under Award Numbers R01AI101047 and R01AI116835 to BZW, and HHSN27220140000C to RWC, SMT and RAT. The content is solely the responsibility of the authors and does not necessarily represent the official views of the National Institutes of Health.

We are grateful to Dr. Jianqin Xu, Shanghai Public Health Clinical Center, Shanghai, China, for providing the lentivrus vector pNL4-3-Luc R-E- and H7N9 HA and NA expressing vectors pVKD-HA and pVKD-NA.

References

1. Zhang H, Wang L, Compans RW, Wang BZ. Universal influenza vaccines, a dream to be realized soon. Viruses. 2014; 6(5):1974–91. [PubMed: 24784572]
2. Krammer F, Palese P. Advances in the development of influenza virus vaccines. Nat Rev Drug Discov. 2015; 14(3):167–82. [PubMed: 25722244]
3. Pushko P, Pujanauski LM, Sun X, Pearce M, Hidajat R, Kort T, et al. Recombinant H7 hemagglutinin forms subviral particles that protect mice and ferrets from challenge with H7N9 influenza virus. Vaccine. 2015; 33(38):4975–82. [PubMed: 26207590]
4. Liu Q, Lu L, Sun Z, Chen GW, Wen Y, Jiang S. Genomic signature and protein sequence analysis of a novel influenza A (H7N9) virus that causes an outbreak in humans in China. Microbes Infect. 2013; 15(6–7):432–9. [PubMed: 23628410]
5. WHO. WHO risk assessment of human infection with avian influenza A(H7N9) virus. 2015. http://www.who.int/influenza/human_animal_interface/influenza_h7n9/RiskAssessment_H7N9_23Feb20115.pdf?ua=1
6. Wong SS, Kaplan B, Zanin M, Debeauchamp J, Kercher L, Crumpton JC, et al. Impact of Adjuvants on the Immunogenicity and Efficacy of Split-Virion H7N9 Vaccine in Ferrets. J Infect Dis. 2015; 212(4):542–51. [PubMed: 25712975]
7. Zhou J, Wang D, Gao R, Zhao B, Song J, Qi X, et al. Biological features of novel avian influenza A (H7N9) virus. Nature. 2013; 499(7459):500–3. [PubMed: 23823727]
8. Jackson LA, Campbell JD, Frey SE, Edwards KM, Keitel WA, Kotloff KL, et al. Effect of Varying Doses of a Monovalent H7N9 Influenza Vaccine With and Without AS03 and MF59 Adjuvants on Immune Response: A Randomized Clinical Trial. JAMA. 2015; 314(3):237–46. [PubMed: 26197184]
9. Couch RB, Patel SM, Wade-Bowers CL, Nino D. A randomized clinical trial of an inactivated avian influenza A (H7N7) vaccine. PLoS One. 2012; 7(12):e49704. [PubMed: 23239968]

10. Cox RJ, Madhun AS, Hauge S, Sjursen H, Major D, Kuhne M, et al. A phase I clinical trial of a PER. C6 cell grown influenza H7 virus vaccine. Vaccine. 2009; 27(13):1889–97. [PubMed: 19368768]
11. Wong SS, Jeevan T, Kercher L, Yoon SW, Petkova AM, Crumpton JC, et al. A single dose of whole inactivated H7N9 influenza vaccine confers protection from severe disease but not infection in ferrets. Vaccine. 2014; 32(35):4571–7. [PubMed: 24950355]
12. Smith GE, Flyer DC, Raghunandan R, Liu Y, Wei Z, Wu Y, et al. Development of influenza H7N9 virus like particle (VLP) vaccine: homologous A/Anhui/1/2013 (H7N9) protection and heterologous A/chicken/Jalisco/CPA1/2012 (H7N3) cross-protection in vaccinated mice challenged with H7N9 virus. Vaccine. 2013; 31(40):4305–13. [PubMed: 23891795]
13. Mayrhofer J, Coulibaly S, Hessel A, Holzer GW, Schwendinger M, Bruhl P, et al. Nonreplicating vaccinia virus vectors expressing the H5 influenza virus hemagglutinin produced in modified Vero cells induce robust protection. J Virol. 2009; 83(10):5192–203. [PubMed: 19279103]
14. Pandey A, Singh N, Sambhara S, Mittal SK. Egg-independent vaccine strategies for highly pathogenic H5N1 influenza viruses. Hum Vaccin. 2010; 6(2):178–88. [PubMed: 19875936]
15. Kelso JM. Safety of influenza vaccines. Curr Opin Allergy Clin Immunol. 2012; 12(4):383–8. [PubMed: 22766619]
16. Weldon WC, Wang BZ, Martin MP, Koutsonanos DG, Skountzou I, Compans RW. Enhanced immunogenicity of stabilized trimeric soluble influenza hemagglutinin. PLoS One. 2010; 5(9) pii: e12466. doi: 10.1371/journal.pone.0012466
17. Petrie JG, Ohmit SE, Johnson E, Truscon R, Monto AS. Persistence of Antibodies to Influenza Hemagglutinin and Neuraminidase Following One or Two Years of Influenza Vaccination. J Infect Dis. 2015; 212(12):1914–22. [PubMed: 26014800]
18. Cox RJ. Correlates of protection to influenza virus, where do we go from here? Hum Vaccin Immunother. 2013; 9(2):405–8. [PubMed: 23291930]
19. Krammer F, Cox RJ. The emergence of H7N9 viruses: a chance to redefine correlates of protection for influenza virus vaccines. Expert Rev Vaccines. 2013; 12(12):1369–72. [PubMed: 24160815]
20. Saczynska V. Influenza virus hemagglutinin as a vaccine antigen produced in bacteria. Acta Biochim Pol. 2014; 61(3):561–72. [PubMed: 25195143]
21. Wang L, Hess A, Chang TZ, Wang YC, Champion JA, Compans RW, et al. Nanoclusters self-assembled from conformation-stabilized influenza M2e as broadly cross-protective influenza vaccines. Nanomedicine. 2014; 10(2):473–82. [PubMed: 23988715]
22. Reed LJ, Muench H. A simple method of estimating fifty percent endpoint. American J Hygiene. 1938; 27:493–7.
23. Qiu C, Huang Y, Zhang A, Tian D, Wan Y, Zhang X, et al. Safe pseudovirus-based assay for neutralization antibodies against influenza A(H7N9) virus. Emerg Infect Dis. 2013; 19(10):1685–7. [PubMed: 24047684]
24. Wang BZ, Quan FS, Kang SM, Bozja J, Skountzou I, Compans RW. Incorporation of membrane-anchored flagellin into influenza virus-like particles enhances the breadth of immune responses. J Virol. 2008; 82(23):11813–23. [PubMed: 18786995]
25. Hirst GK. The Quantitative Determination of Influenza Virus and Antibodies by Means of Red Cell Agglutination. J Exp Med. 1942; 75(1):49–64. [PubMed: 19871167]
26. Reber A, Katz J. Immunological assessment of influenza vaccines and immune correlates of protection. Expert Rev Vaccines. 2013; 12(5):519–36. [PubMed: 23659300]
27. Belshe RB, Gruber WC, Mendelman PM, Mehta HB, Mahmood K, Reisinger K, et al. Correlates of immune protection induced by live, attenuated, cold-adapted, trivalent, intranasal influenza virus vaccine. J Infect Dis. 2000; 181(3):1133–7. [PubMed: 10720541]
28. Noah DL, Hill H, Hines D, White EL, Wolff MC. Qualification of the hemagglutination inhibition assay in support of pandemic influenza vaccine licensure. Clin Vaccine Immunol. 2009; 16(4): 558–66. [PubMed: 19225073]
29. Food and drug administration. Guidance for industry: clinical data needed to support the licensure of seasonal inactivated influenza vaccines. US Food and Drug Administration; Rockville, MD: 2007. http://www.fda.gov/BiologicsBloodVaccines/GuidanceComplianceRegulatoryInformation/Guidances/Vaccines/ucm074794.htm#iii

30. Neumann G, Noda T, Kawaoka Y. Emergence and pandemic potential of swine-origin H1N1 influenza virus. Nature. 2009; 459(7249):931–9. [PubMed: 19525932]
31. De Groot AS, Moise L, Liu R, Gutierrez AH, Terry F, Koita OA, et al. Cross-conservation of T-cell epitopes: now even more relevant to (H7N9) influenza vaccine design. Hum Vaccin Immunother. 2014; 10(2):256–62. [PubMed: 24525618]
32. De Groot AS, Ardito M, Terry F, Levitz L, Ross T, Moise L, et al. Low immunogenicity predicted for emerging avian-origin H7N9: implication for influenza vaccine design. Hum Vaccin Immunother. 2013; 9(5):950–6. [PubMed: 23807079]
33. Chua BY, Brown LE, Jackson DC. Considerations for the rapid deployment of vaccines against H7N9 influenza. Expert Rev Vaccines. 2014; 13(11):1327–37. [PubMed: 25017993]
34. Bart SA, Hohenboken M, Della Cioppa G, Narasimhan V, Dormitzer PR, Kanesa-Thasan N. A cell culture-derived MF59-adjuvanted pandemic A/H7N9 vaccine is immunogenic in adults. Sci Transl Med. 2014; 6(234):234ra55.
35. Wohlfart S, Gelperina S, Kreuter J. Transport of drugs across the blood-brain barrier by nanoparticles. J Control Release. 2012; 161(2):264–73. [PubMed: 21872624]
36. Park K. Transport across the blood-brain barrier using albumin nanoparticles. J Control Release. 2009; 137(1):1. [PubMed: 19427883]
37. Lamm ME. Interaction of antigens and antibodies at mucosal surfaces. Annu Rev Microbiol. 1997; 51:311–40. [PubMed: 9343353]
38. Neutra MR, Kozlowski PA. Mucosal vaccines: the promise and the challenge. Nat Rev Immunol. 2006; 6(2):148–58. [PubMed: 16491139]
39. Vyas SP, Gupta PN. Implication of nanoparticles/microparticles in mucosal vaccine delivery. Expert Rev Vaccines. 2007; 6(3):401–18. [PubMed: 17542755]
40. Cone RA. Barrier properties of mucus. Advanced Drug Delivery Reviews. 2009; 61(2):75–85. [PubMed: 19135107]

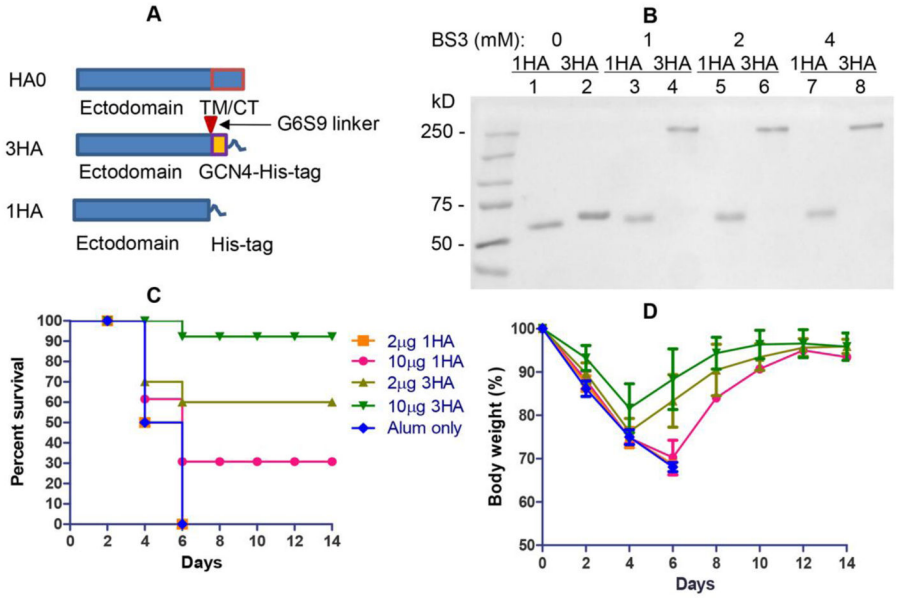

Figure 1. characterization and immunogenicity of soluble trimeric H7N9 HA

(A) Schematic diagram of constructs expressing full-length HA (HA0), trimeric HA (3HA) and monomeric HA (1HA). In 3HA, a 6-glycine-9-serine linker was inserted between the HA ectodomain and tGCN4. (B) Western blotting analysis of purified recombinant HA and 3HA. Proteins were crosslinked using BS3 crosslinking reaction at relative concentration (0, 1, 2, and 4) respectively. After the crosslinking reaction, protein samples (0.2 μg protein) were analyzed by Western blot. (C) Mouse survival post-challenge. Mouse groups (12 mice per group) were intramuscularly (i.m.) immunized twice with 2 or 10 μg of 1HA or 3HA adjuvanted with Alum according to the manufacturer's instruction. (D) Mouse bodyweight change post-challenge. Data are expressed by the mean percent change ± SEM (n = 12).

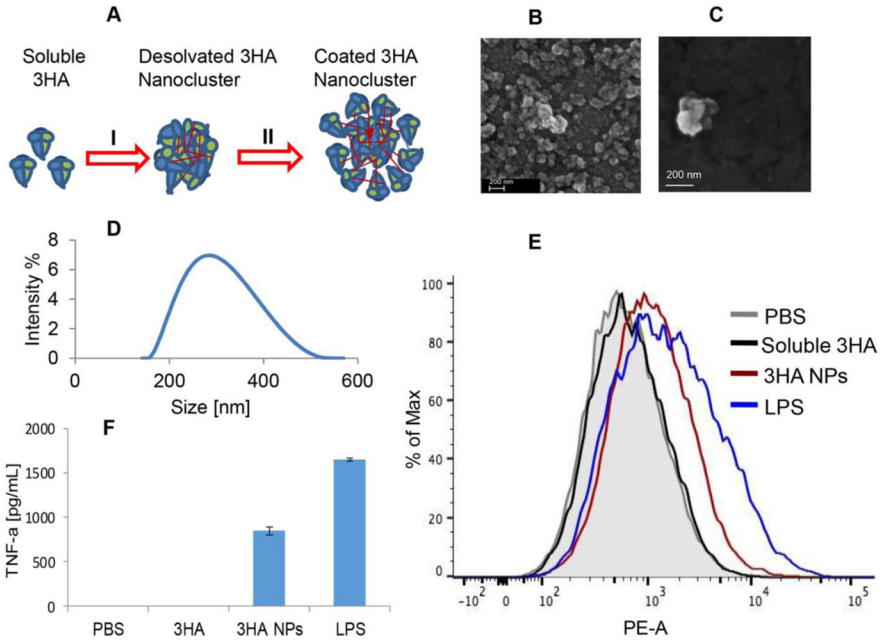

Figure 2. Generation and characterization of coated (two-layer) H7N9 3HA nanoclusters

(A) Schematic diagram of coated (double-layer) 3HA nanocluster generation. H7N9 3HA proteins were assembled into desolvated protein nanoclusters (process I). An additional layer of 3HA molecules was crosslinked onto the desolvated nanoparticle surfaces via DTSSP crosslinking (process II). (B, C) Scanning electron microscopy of coated 3HA nanoclusters. Coated 3HA images were obtained with a Zeiss Ultra60 FE scanning electron microscope. (D) Size distribution of coated 3HA nanoclusters. DLS data were acquired with a Malvern Zetasizer Nano ZS. (E) CD86 expression on DC cell surfaces. JAWS II murine DCs were treated with soluble 3HA (3HA), 3HA nanoclusters (3HA NPs), LPS (positive control) and PBS (negative control). (F) TNF-α secretion by treated DC cells.

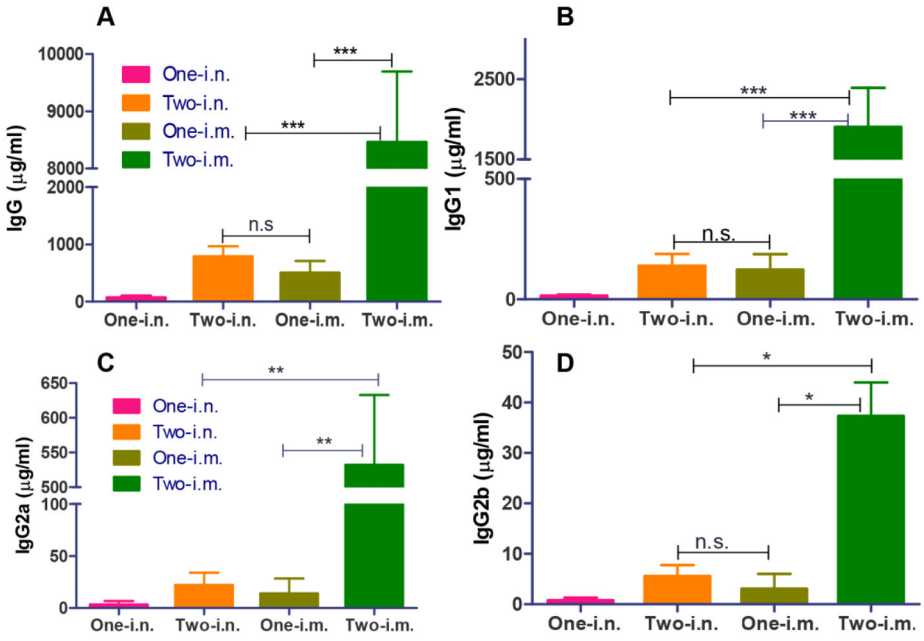

Figure 3. Serum antibody responses induced by 3HA nanoclusters

Mice were immunized once or twice through i.m. and i.n. routes, respectively. Immune sera were diluted 1000-fold and then used for ELISA analysis. Data are depicted as the mean ± SD (n=7–8). (A) Serum total IgG level. (B) Serum IgG1. (C) Serum IgG2a. (D) Serum IgG2b.

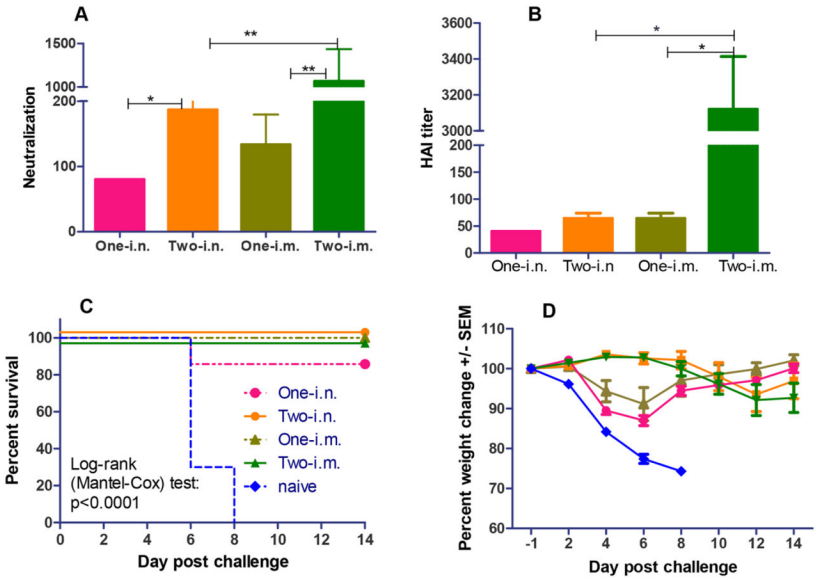

Figure 4. Antibody neutralization and HAI titers of immune sera, and protection against live virus challenge induced by 3HA nanoclusters

A) Serum antibody neutralizing activity. Immune sera were diluted 2-fold stepwise for assays of both neutralization and HAI titers. Data represent mean ± SEM (n=7–8). (B) Immune serum HAI titers. (C) Mouse survival. Immunized mice were challenged with A/Anhui/1/2013 (H7N9) virus as designed in Methods. (D) Mouse bodyweight changes. Mouse mortality and body weight changes postchallenge were monitored daily for two weeks. Data were expressed by the mean percentage change ± SEM.

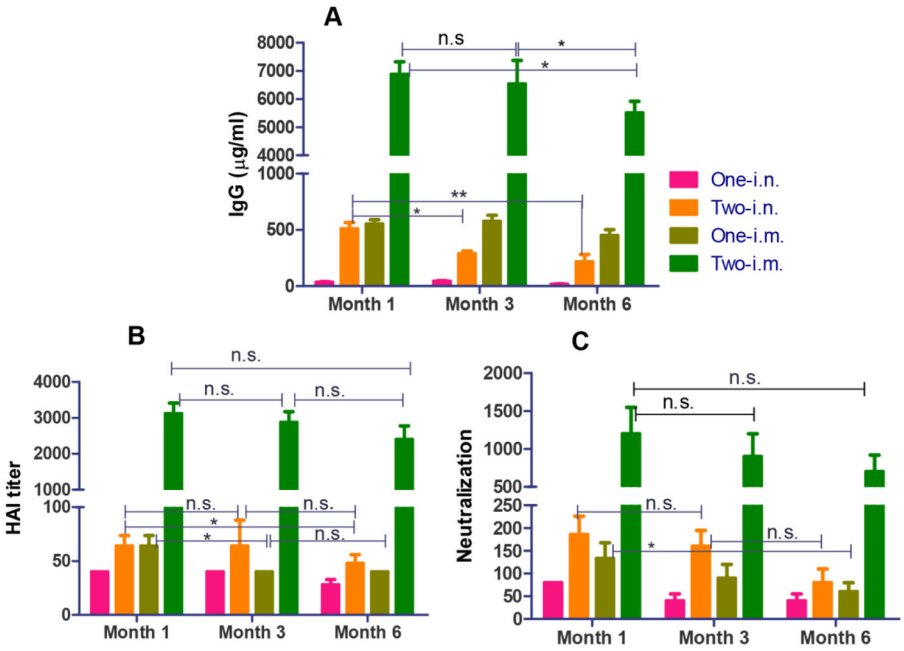

Figure 5. Long-lasting protective antibody responses induced by 3HA nanoclusters

Antibody responses were measured in immune sera at time points of 1, 3 and 6 months after immunization. (A) Immune serum IgG levels. (B) HAI titers. (C) Serum antibody neutralizing activity.